



LAWRENCE  
LIVERMORE  
NATIONAL  
LABORATORY

# XRD and NMR investigation of Ti-compound formation in solution-doping of sodium aluminum hydrides: Solubility of Ti in NaAlH<sub>4</sub> crystals grown in THF

E. H. Majzoub, J. L. Herberg, R. Stumpf, S.  
Spangler, R. S. Maxwell

November 9, 2004

Journal of Alloys and Compounds

## **Disclaimer**

---

This document was prepared as an account of work sponsored by an agency of the United States Government. Neither the United States Government nor the University of California nor any of their employees, makes any warranty, express or implied, or assumes any legal liability or responsibility for the accuracy, completeness, or usefulness of any information, apparatus, product, or process disclosed, or represents that its use would not infringe privately owned rights. Reference herein to any specific commercial product, process, or service by trade name, trademark, manufacturer, or otherwise, does not necessarily constitute or imply its endorsement, recommendation, or favoring by the United States Government or the University of California. The views and opinions of authors expressed herein do not necessarily state or reflect those of the United States Government or the University of California, and shall not be used for advertising or product endorsement purposes.

# XRD and NMR investigation of Ti-compound formation in solution-doping of sodium aluminum hydrides: Solubility of Ti in NaAlH<sub>4</sub> crystals grown in THF.

E.H. Majzoub<sup>a\*</sup>, J.L. Herberg<sup>b</sup>, R. Stumpf<sup>a</sup>, S. Spangler<sup>a</sup>, R.S. Maxwell<sup>b</sup>

<sup>a</sup>Sandia National Laboratories, P.O. Box 969, Livermore, CA, 94551 USA

<sup>b</sup>Lawrence Livermore National Laboratories, P.O. Box 808, Livermore, CA, 94551 USA

August 23, 2004

## Abstract

Sodium aluminum hydrides have gained attention due to their high hydrogen weight percent (5.5% ideal) compared to interstitial hydrides, and as a model for hydrides with even higher hydrogen weight fraction. The purpose of this paper is to investigate the Ti-compounds that are formed under solution-doping techniques, such as wet doping in solvents such as tetrahydrofuran (THF). Compound formation in Ti-doped sodium aluminum hydrides is investigated using x-ray diffraction (XRD) and magic angle spinning (MAS) nuclear magnetic resonance (NMR). We present lattice parameter measurements of crushed single crystals, which were exposed to Ti during growth. Rietveld refinements indicate no lattice parameter change and thus no solubility for Ti in NaAlH<sub>4</sub> by this method of exposure. In addition, x-ray diffraction data indicate that no Ti substitutes in NaH, the final decomposition product for the alanate. Reaction products of completely reacted (33.3 at. %-doped) samples that were solvent-mixed or mechanically milled are investigated. Formation of TiAl<sub>3</sub> is observed in mechanically milled materials, but not solution mixed samples, where bonding to THF likely stabilizes Ti-based nano-clusters. The Ti in these clusters is activated by mechanical milling.

## 1 Introduction

The decomposition of sodium alanate was first shown to be kinetically enhanced and reversible by Bogdanovic and coworkers by the addition of Ti-dopant [1, 2]. The decomposition proceeds as



where the aluminum is known to agglomerate into bulk form, which is easily visible in x-ray diffraction of decomposed material. The rate of these reactions is enhanced by several orders of magnitude by the addition of a Ti-dopant, which lowers the activation energy of the absorption and desorption processes [3]. However, the method by which the Ti-dopant works is still not understood [4, 5]. The location of dopant Ti in sodium alanate has become the leading question in the study of this complex-hydride system. Identifying the compounds in which the Ti is located after the doping procedure may help to explain the enhanced reaction kinetics.

There is some evidence to suggest that Ti may substitute in the alanate structure resulting in lattice parameter changes upon doping through mechanical milling [6]; however, the absence of a lattice parameter standard in these studies casts doubt on the validity of the results obtained. In addition, others have been unable to produce similar results [5]. Upon heating and decomposition of Ti-doped samples, a shoulder is observed in prominent aluminum reflections, and has been interpreted as Ti incorporation into bulk Al [7]. This suggests, with the Ti-Al binary phase diagram and the fact that Ti-Al line compounds have favorable formation energies, that Ti-Al compounds are likely to form in this system [4].

There is a striking difference in hydrogen sorption rates when doping through different techniques. For example, mechanically milling Ti-halide dopants with NaAlH<sub>4</sub> powder results in rapid initial kinetics, while the same milling with TiH<sub>2</sub>, or TiAl<sub>3</sub> as a dopant results in very slow initial kinetics. However, it has been shown that samples prepared through mechanical milling of NaAlH<sub>4</sub> and TiH<sub>2</sub> show hydrogen absorption rates that increase upon cycling from extremely poor, to rates comparable to doping with Ti-halides [8]. Doping with Ti nano-clusters has been demonstrated and results in faster absorption reaction kinetics than doping with Ti-halides [9, 10]. The Ti nano-clusters in the work of Fichtner, *et al.*, and Bogdanovic, *et al.*, were prepared in solutions of tetrahydrofuran (THF).

In this paper, we (1) demonstrate that no lattice parameter changes are seen in NaAlH<sub>4</sub> crystals grown in saturated solutions of THF, (2) show that lattice parameter changes seen in NaH, when doping with TiF<sub>3</sub> are due to fluorine substitution in the NaH lattice, and (3) indicate the differences between some of the compounds formed in solvent-free production of active materials, and those prepared through TiCl<sub>3</sub> doping in THF. Samples prepared by doping in THF did not show hydrogen

---

\*Corresponding author. Tel.: +1-925-294-2498; fax: +1-925-294-3410. *E-mail address*: ehmajzo@sandia.gov

sorption activity unless mechanically milled. This information may help to indicate the nature of the compounds which are active by different doping procedures.

Growth of large crystals (of order 0.5 mm) of  $\text{NaAlH}_4$  was performed for our x-ray study because small changes in structure factors are more likely to be observable in well ordered crystals as opposed to the more pragmatic mechanically milled materials. In addition, mechanical milling is known to produce metastable structures, and we were interested in determining ground state structures of Ti substitution defects, if they were present.

## 2 Experimental Details

The samples prepared for this work are listed in Table (1). Single crystal samples of  $\text{NaAlH}_4$  were grown by solvent evaporation from *Sigma Aldrich* 1 M solutions of  $\text{NaAlH}_4$  in THF. These samples are referred to as “pure- $\text{NaAlH}_4$ ”, or ( $S_1$ ). *NIST* powdered silicon was added as lattice constant standard for x-ray diffraction refinements. Samples referred to as “Ti-exposed,” or ( $S_2$ ), were prepared as the pure single crystals, with  $\text{TiCl}_3$  added to the solution at 4 at.%, with respect to the amount of alanate in solution, before the solvent evaporation. The single crystal samples were crushed by hand in a mortar and pestle for diffraction and NMR spectra. Alternatively to ( $S_2$ ) samples, rapidly dried 4 at.% doped samples, prepared in THF, resulted in fine powders and are referred to as ( $S_{3a}$ ). Samples of ( $S_{3a}$ ) were also mechanically milled for some sorption experiments, and are referred to as ( $S_{3b}$ ).

In addition, 33.3 at.% doped samples ( $3\text{NaAlH}_4 + \text{TiCl}_3$ ) were prepared. This ratio was chosen so that all of the alanate would be consumed leading to larger quantities of reaction products. Samples prepared for study are referred to as 33.3 at.% doped “solvent” ( $S_4$ ) and “solvent-free” ( $S_5$ ). The solvent-free samples were prepared by mechanical milling of  $\text{NaAlH}_4$  powder and  $\text{TiCl}_3$  powder in a SPEX mill as described elsewhere [4]. The solution-mixed samples were prepared in THF in an argon-filled dry box by the addition of 0.257 g of  $\text{TiCl}_3$  to 5 cc of 1 M  $\text{NaAlH}_4$  in THF, which was allowed to evaporate at room temperature in an argon dry box.

Sample	Solvent	Ti-precursor	at.% dopant	Form	Milled
$S_1$	THF	none	0	crushed crystal	no
$S_2$	THF	$\text{TiCl}_3$	4	crushed crystal	no
$S_{3a}$	THF	$\text{TiCl}_3$	4	fine powder	no
$S_{3b}$	THF	$\text{TiCl}_3$	4	fine powder	yes
$S_4$	THF	$\text{TiCl}_3$	33	fine powder	no
$S_5$	none	$\text{TiCl}_3$	33	fine powder	yes

Table 1: Samples used in this work.

X-ray diffraction was performed using  $\text{Cu-K}_\alpha$  radiation on a *Scintag XDS-2000* using Bragg-Brentano geometry and airless sample holders, using a step size of  $0.02^\circ 2\theta$ , and a count time of 0.5 s. X-ray fluorescence spectra were collected on a KEVEX Omicron using a Cu x-ray source operated at 50 kV and 1 mA, with a  $50\ \mu\text{m}$  aperture and 100 sec collection time.

Hydrogen sorption experiments were performed on sample sizes of about 2 g, which were transferred to a sealed stainless-steel sample vessel and connected to a pressure, and temperature-controlled hydrogen manifold. All steps for sample preparation and transfer into the reactor vessel occurred inside an Ar glove box with oxygen levels below 3 ppm.

MAS NMR measurements were performed on a Bruker Avance 400WB spectrometer with a magnetic field of 9.4 T. This gives a resonance frequency of 104.25 MHz for  $^{27}\text{Al}$  (spin  $\frac{5}{2}$ ) and 105.84 MHz for  $^{23}\text{Na}$  (spin  $\frac{3}{2}$ ). The samples were packed in 4 mm MAS rotors inside an Ar glove box with oxygen levels below 3 ppm. Spinning rates of 9 kHz and 12 kHz were used. The Free Induction Decay (FID) spectra were taken with a single excitation pulse. For both  $^{27}\text{Al}$  and  $^{23}\text{Na}$  NMR, a short pulse and small flip angle was used ( $^{27}\text{Al}$  MAS NMR with a 8 degree pulse width of  $0.2\ \mu\text{s}$  and  $^{23}\text{Na}$  MAS NMR with a 8 degree pulse width of  $0.2\ \mu\text{s}$ ). The  $^{27}\text{Al}$  spectra were referenced to aqueous solutions of  $\text{Al}(\text{NO}_3)_3$  and  $^{23}\text{Na}$  was referenced to aqueous solutions of  $\text{NaNO}_3$ .

## 3 Rietveld Refinements of pure and Ti-exposed $\text{NaAlH}_4$

The lattice parameters of undoped and 4 at.% Ti-exposed single crystals, samples ( $S_4$ ) and ( $S_5$ ), were determined by Rietveld refinement of x-ray diffraction from gently powdered samples using SIMREF 2.6 [11]. Peak shapes of the x-ray data were fit using the pseudo-Voigt profile containing a mixture of Gaussian and Lorentzian line shapes, as shown in Figure (1). The Bragg residuals for  $\text{NaAlH}_4$  for the pure and Ti-exposed samples were 14% and 6.8%, respectively. Overall refinement residuals, including the silicon peaks are shown in Table (2). The definition of the residuals  $R_p$ ,  $R_{wp}$ ,  $R_e$ , and  $R_{Bragg}$ , can be found in the SIMREF technical manual [11]. The lattice constants from the fit to the Ti-exposed sample yielded  $a = 5.0238\ \text{\AA}$  and  $c = 11.3506\ \text{\AA}$ . The lattice constants from a pure  $\text{NaAlH}_4$  crushed single crystal yielded  $a = 5.0238\ \text{\AA}$  and  $c = 11.3504\ \text{\AA}$ , indicating that there is no observable shift in the lattice constants due to the exposure of Ti *by this method*. If we assume that Ti substitution would shift the lattice parameters, therefore Ti appears to be essentially insoluble in  $\text{NaAlH}_4$ .

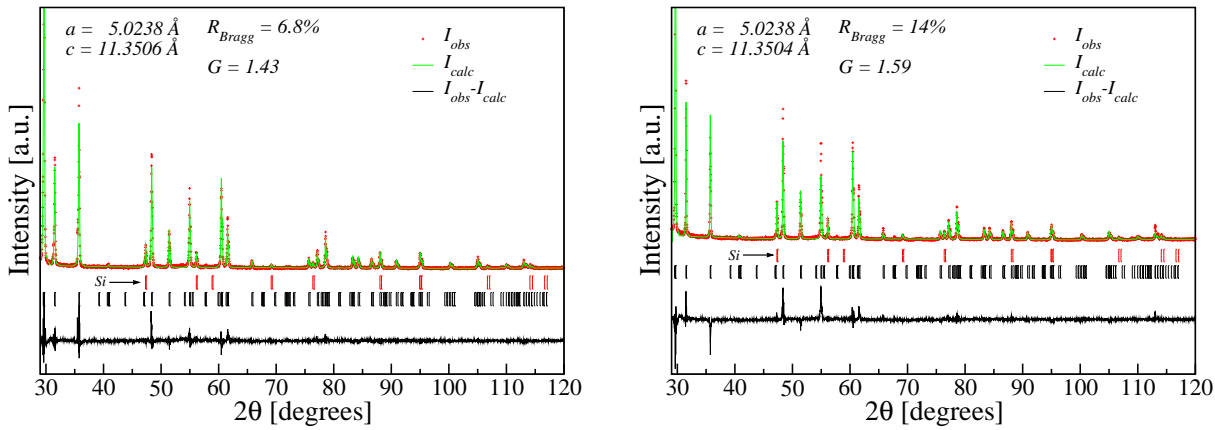


Figure 1: Rietveld refinement of Ti-exposed crushed single crystals. The lattice parameters show no change within 0.0002 Å, suggesting that no titanium is introduced into the lattice with this method of doping.

These results are in agreement with total energy calculations indicating that Ti substitution on Na or Al sites is energetically unfavorable in perfect NaAlH<sub>4</sub> at realistic chemical potentials [12].

Table 2: Lattice parameters and overall refinement residuals for the refinements of pure and Ti-exposed NaAlH<sub>4</sub>.

Data Set	a [Å]	c [Å]	$R_p$	$R_{wp}$	$R_{exp}$	$(N - P)$	$S$
pure	5.0238	11.3504	0.143	0.184	0.120	5051	1.59
Ti-exposed	5.0238	11.3506	0.126	0.170	0.120	5049	1.43

Our measurements also suggest that Ti does not substitute in NaH, the final hydride decomposition product in Eq. (1). X-ray diffraction of annealed samples of NaH, mechanically milled with TiCl<sub>3</sub>, show no lattice parameter changes in diffraction data greater than 0.04%. However, lattice parameter changes of the NaH observed upon mechanical mixing of TiF<sub>3</sub> and NaH were observed, and are consistent with fluorine substitution in the NaH lattice, as the lattice parameter shifts linearly between bulk NaH and bulk NaF, as shown in Figure (2). This is in contrast to doping with Cl-containing compounds, where NaCl is evidenced even at small doping levels.

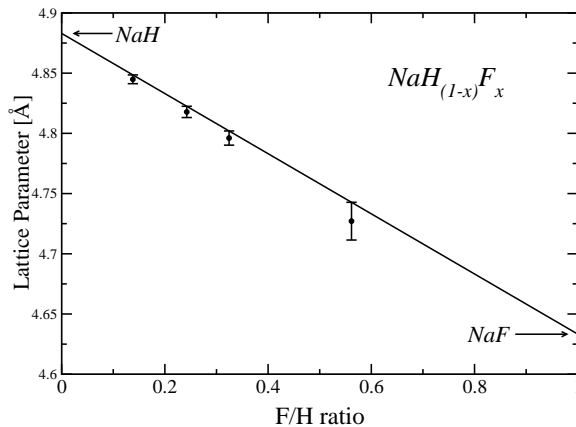


Figure 2: Lattice parameter of annealed NaH after mechanical milling with TiF<sub>3</sub>, where the F/H ratio is given on the x-axis. The lattice parameter shifts linearly from that of NaH toward NaF with increasing F content.

## 4 Compound formation in 33.3 at. % Ti-doped NaAlH<sub>4</sub>

In order to determine the possible structures in which Ti may be residing, the dopant level was increased to a large enough value that all the available alanate is consumed, leaving only NaCl, and Ti-Al-H reaction products. X-ray diffraction of mechanically milled samples of 33.3 at. % doped material (S<sub>5</sub>) indicate that TiAl<sub>3</sub> formation is likely [4]. However, the same dopant ratio applied in a solution of THF (S<sub>4</sub>) shows no indication of TiAl<sub>3</sub>. X-ray diffraction in Figure (3a) shows that no bulk Ti or TiAl<sub>3</sub> is formed in solution mixing of NaAlH<sub>4</sub> and TiCl<sub>3</sub>. The only observed peaks in our experiments correspond

to bulk Al, and NaCl. The presence of Ti is clearly indicated in x-ray fluorescence of the solution-mixed sample, despite the absence of any indication of bulk (hcp) Ti or  $\text{TiAl}_3$  in x-ray diffraction. There is an indication of an amorphous or low coherence length phase in the x-ray spectrum between 15-40 degrees  $2\theta$ , shown as a very broad increase in the background intensity in the inset to Figure (3b). The Scherrer particle size equation yields a calculated coherence length of about 7 Å from the FWHM of this background intensity.

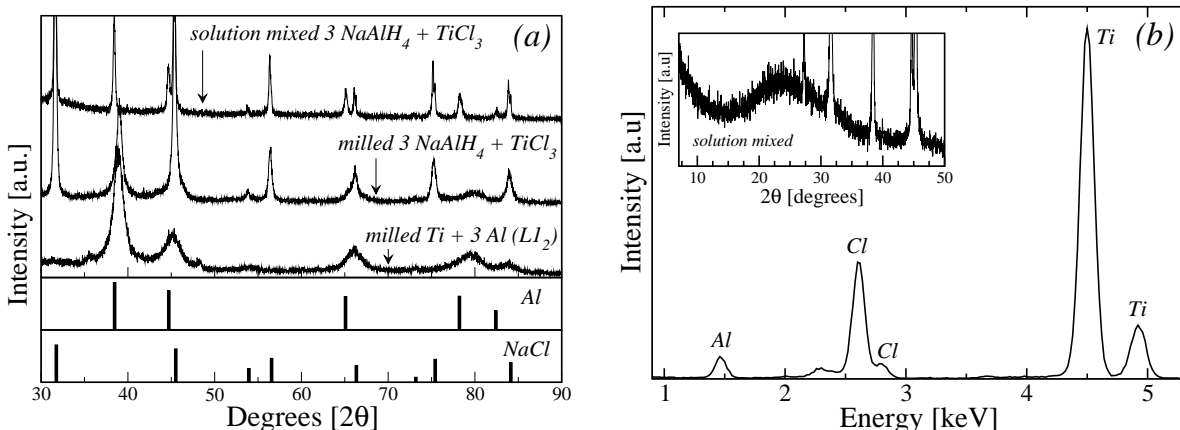
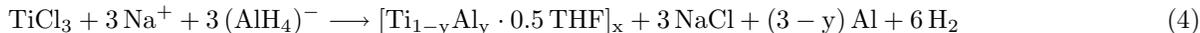


Figure 3: X-ray diffraction (a) of THF solution-mixed, and mechanically-milled  $3 \text{NaAlH}_4 + \text{TiCl}_3$ . Metastable  $\text{TiAl}_3$ , in the  $L_2$  structure is shown for reference. Diffraction data shows no Ti-compounds, but the presence of Ti in the material is evidenced by the clear XRF signal (b), which, together with the inset XRD showing a wide peak of intensity at low angle, indicates the presence of Ti in either nano-particle or amorphous compounds.

Some of the possible reactions occurring in the THF solvent include:



The free energies of formation for some Ti-Al and Ti-H compounds are shown in Table (3). The difference in Gibbs' free energy for reactions (2) and (3) is about 50 kJ/mol, favoring the formation of  $\text{TiAl}_3$ . Therefore, in the solvent-mixed samples,

Compound	$\Delta G_f^\circ$ [kJ/mol]
TiAl	-72
TiH <sub>2</sub>	-86
TiAl <sub>3</sub>	-136
Al <sub>2</sub> O <sub>3</sub>	-1582
TiO <sub>2</sub>	-889

Table 3: Formation energies for possible Ti-Al-H compounds.

the Ti may form an unknown  $\text{TiAl}_x\text{H}_y$  compound, or a  $\text{Ti}_{(1-y)}\text{Al}_y$  nano-particle colloid, due to the similarity in the solution reactions used to produce the Ti nano-particles in the work of Bogdanovic and Fichtner. Three experimental results suggest the latter. First, the presence of hydrogen is indicated by proton NMR in the solvent mixed samples, suggesting that residual THF may be present. Second, the sorption kinetics of the 4 at. %-doped samples ( $S_{3a}$ ) and ( $S_{3b}$ ), solution-mixed in THF, indicate that mechanical milling of the samples was required for activity, in agreement with the work of Bogdanovic and Fichtner [10, 9]. (The sample not milled after evaporating the THF was initially desorbed at 160 °C into a vacuum, releasing 53 % of its reversible hydrogen over a 1.5 hr period. A subsequent absorption showed no hydrogen uptake, over a 2 hr period, at pressures up to 82 bar at a temperature of about 95 °C. In contrast, the sample which was mechanically milled after drying, desorbed about 73 % of its reversible hydrogen over a 1.5 hr period at 160 °C. A subsequent absorption of the milled sample at about 85 °C and 85 bar over 2 hrs indicated an absorption of over 90 % of the hydrogen which was initially desorbed.) Finally, x-ray diffraction and  $^{27}\text{Al}$  NMR data show bulk Al, not TiAl or  $\text{TiAl}_3$ .

$^{27}\text{Al}$  MAS NMR spectra of the four doped  $\text{NaAlH}_4$  materials are shown in Figure (4), with peak positions given in Table (4). The spectra for sample ( $S_2$ ) shown in Figure (4a), is characterized by a peak at 94.6 ppm due to  $\text{NaAlH}_4$ . The spectrum of sample ( $S_{3a}$ ) shown in Figure (4b) is characterized by three distinct  $^{27}\text{Al}$  NMR resonances: one at 1640 ppm, assigned to metallic aluminum; one at approximately -42.6 ppm, assigned to  $\text{Na}_3\text{AlH}_6$ ; and one at 94.2 ppm, assigned to  $\text{NaAlH}_4$ . These assignments were made based on comparisons to pure materials (data not shown), and previous findings on

similar materials [5]. The  $^{27}\text{Al}$  MAS spectra for samples ( $S_4$ ) and ( $S_5$ ) are shown in Figures (4c) and (4d), respectively. It is clear from the  $^{27}\text{Al}$  MAS NMR spectra that the aluminum speciation is dramatically affected by the processing methods. Sample ( $S_4$ ) has two distinct peaks: metallic aluminum at 1641 ppm and a series of overlapping resonances at 8.4 ppm, 35.5 ppm, and 63.6 ppm, assigned to six, five, and four coordinate aluminum-oxygen species, respectively, in  $\text{Al}_2\text{O}_3$  [13]. To confirm that this peak did not represent any  $\text{AlH}_4$  species, we performed  $^{27}\text{Al}\{^1\text{H}\}$  MAS NMR experiments and observed no significant narrowing of the  $\text{Al}_2\text{O}_3$  resonances with decoupling, which we did observe in the  $\text{NaAlH}_4$  peak for sample ( $S_2$ ).  $^{27}\text{Al}$  MQ MAS, to be discussed in future publications, was also performed on this sample and shows distinct isotropic quadrupolar shifts that show fairly ordered sites for the different  $\text{Al}_2\text{O}_3$  species, including 1) octahedral 0–10 ppm, 2) pentacoordinate around 30 ppm, and 3) tetrahedral 40–80 ppm [14]. This means that there is either a small distribution of quadrupolar coupling or an amorphous unknown structure. In X-ray diffraction, the coherence length of crystals is related to the peak width. This means that nano-sized crystals are represented by extremely broad peaks in the background. Since the X-ray diffraction does not show any indication of crystalline  $\text{Al}_2\text{O}_3$  and the pentacoordinate  $\text{Al}_2\text{O}_3$  exists in the  $^{27}\text{Al}$  MQMAS data, this indicates that  $\text{Al}_2\text{O}_3$  are in the form of nano-clusters of  $\text{Al}_2\text{O}_3$  and possess sharp peaks in the  $^{27}\text{Al}$  MQ MAS data due to the  $\text{Al}_2\text{O}_3$  quadrupolar interaction with electric field gradient on the surface of this material [13]. This result indicates that this peak is not due to  $\text{AlH}_4$  clusters, which would have large Al-H dipolar couplings due to the short Al-H bonding. The presence of  $\text{Al}_2\text{O}_3$  in sample ( $S_4$ ) may suggest contamination during processing, or strong coordination between the Al and THF molecules. The  $^{27}\text{Al}$  NMR spectra of sample ( $S_5$ ) shown in Figure (4d) shows four resonances: two at approximately

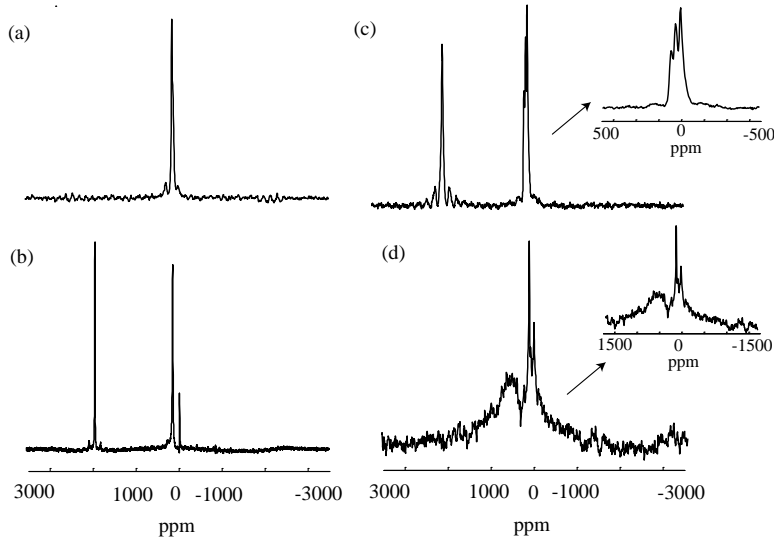


Figure 4:  $^{27}\text{Al}$  MAS NMR spectra of samples (a)  $S_2$ , (b)  $S_{3a}$ , (c)  $S_4$ , and (d)  $S_5$ .

Table 4:  $^{27}\text{Al}$  NMR lines in [ppm] of the detected compounds in each sample.

Compound	$S_2$	$S_3$	$S_4$	$S_5$
$\text{NaAlH}_4$	$94.6 \pm 0.5$	$94.2 \pm 0.5$		
$\text{Na}_3\text{AlH}_6$		$-42.6 \pm 0.2$		
Al metal		$1640.0 \pm 0.9$	$1641.0 \pm 0.9$	$1640.0 \pm 0.9$
$\text{TiAl}_3$				$664 \pm 0.4$
$\text{Al}_2\text{O}_3$ (6-fold)			$8.4 \pm 0.1$	
$\text{Al}_2\text{O}_3$ (5-fold)			$35.5 \pm 0.2$	
$\text{Al}_2\text{O}_3$ (4-fold)			$63.6 \pm 0.3$	

10 ppm and 103 ppm, with respective line widths of 19 ppm and 30 ppm, a broad resonance at approximately 664 ppm, and a metallic aluminum resonance at 1640 ppm. The extremely broad line shape of the 664 ppm resonance suggests the presence of some amorphous or nanoclustered  $\text{TiAl}_3$ . Figure (5) directly compares the  $^{27}\text{Al}$  MAS NMR spectra of pure  $\text{TiAl}_3$  in the  $L1_2$  metastable structure (preparation of this phase is described elsewhere [4]) and ( $S_5$ ). These line shapes are extremely similar and indicate that there may be  $\text{TiAl}_3$  in sample ( $S_5$ ). The differences in line shape might be a result of the small differences in the local environments of Al in the  $\text{TiAl}_3$ . This observation also agrees with results from the x-ray diffraction studies above, which show that in ( $S_5$ ) samples the formation of  $\text{TiAl}_3$  is likely. However, the  $^{27}\text{Al}$  MAS NMR of sample ( $S_4$ ) shows no presence of  $\text{TiAl}_3$ , and only indicates the presence of metallic aluminum and  $\text{Al}_2\text{O}_3$ .

$^{23}\text{Na}$  MAS NMR spectra are shown in Figure (6), with peak positions given in Table (5). Figure (6a) shows a spectrum with a peak at -9.4 ppm from sample ( $S_2$ ), and indicates only the presence of  $\text{NaAlH}_4$  in this sample. The spectra of sample

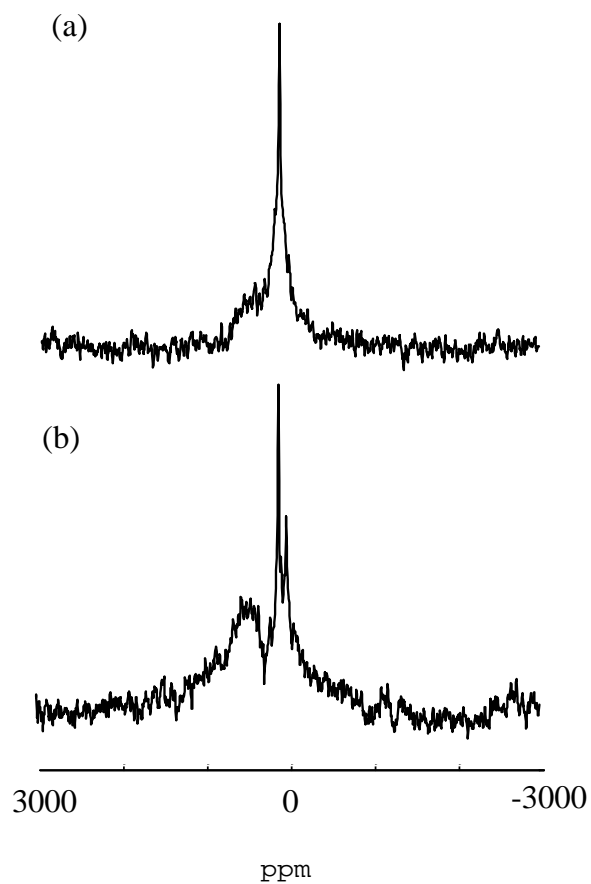


Figure 5:  $^{27}\text{Al}$  MAS NMR spectra of (a)  $\text{TiAl}_3$  in the  $\text{L1}_2$  structure, and (b) sample  $\text{S}_5$ .

Table 5:  $^{23}\text{Na}$  NMR lines in [ppm] of the detected compounds in each sample.

Compound	$\text{S}_2$	$\text{S}_3$	$\text{S}_4$	$\text{S}_5$
$\text{NaCl}$		$7.2 \pm 0.3$	$7.0 \pm 0.3$	$6.8 \pm 0.3$
$\text{NaAlH}_4$	$-9.4 \pm 0.3$	$-9.4 \pm 0.3$		
$\text{Na}_3\text{AlH}_6$		$22.9 \pm 0.4$		

( $S_{3a}$ ) is shown Figure (6b), in which three resonances were observed: one at -9.4 ppm due to  $\text{NaAlH}_4$ , one at 22.9 ppm, indicating the presence of  $\text{Na}_3\text{AlH}_6$ , and one at 7.2 ppm, which indicates the presence of  $\text{NaCl}$ . Spectra from samples ( $S_4$ ) and ( $S_5$ ) are not shown, and indicate the presence of only  $\text{NaCl}$ , as expected. Proton NMR (not shown) also indicates that

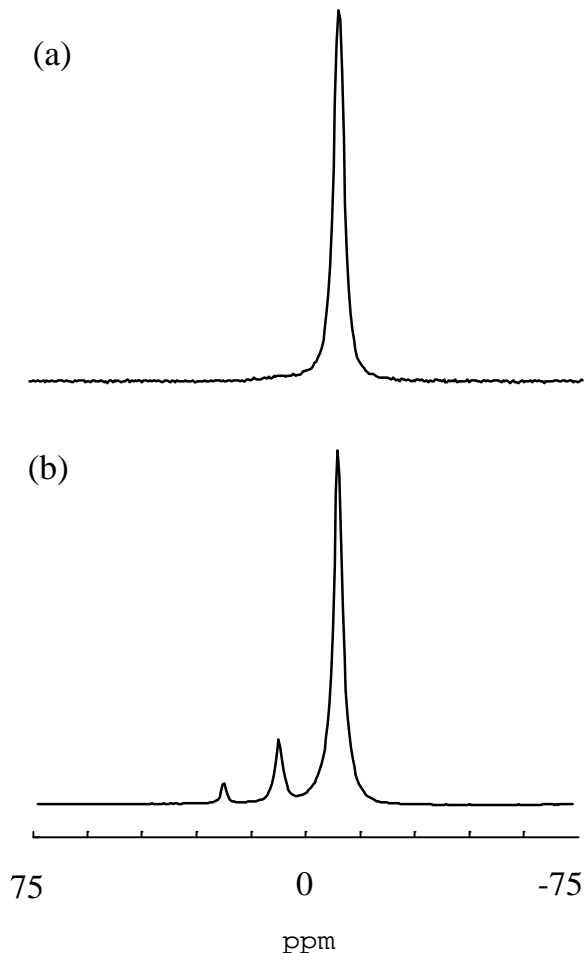


Figure 6:  $^{23}\text{Na}$  MAS NMR spectra of samples (a)  $S_2$ , and (b)  $S_{3a}$ .

hydrogen is present in the solvent-doped samples, but this may be due to residual THF, suggesting nano-particle formation as discussed above. However, a possible candidate for the Ti compound in the solvent-doped sample is  $\text{TiH}_2$ .

## 5 Conclusions

X-ray diffraction of  $\text{NaAlH}_4$  crystals grown from saturated THF solutions containing  $\text{TiCl}_3$ , and annealing studies of  $\text{TiCl}_3$ -doped  $\text{NaH}$ , indicate no solubility for Ti in the  $\text{NaAlH}_4$  or  $\text{NaH}$  lattices, respectively. Lattice parameter changes observed in  $\text{NaH}$  in  $\text{TiF}_3$  doped samples are shown to be fluorine substitution into the  $\text{NaH}$  lattice. The reaction products in doped  $\text{NaAlH}_4$  depend on the method of preparation. Mechanical milling and solution mixing are shown to result in different Ti-compounds. The formation of  $\text{TiAl}_3$  is indicated in mechanical milling, but does not appear to form in solution mixed samples, as indicated by x-ray diffraction, and  $^{27}\text{Al}$  MAS NMR. The  $^{27}\text{Al}$  MAS NMR of THF-solution mixed samples indicates aluminum in bulk and possibly  $\text{Al}_2\text{O}_3$  on surfaces, which may be consistent with Ti-Al nano-clusters where oxygen in the THF molecule is coordinated with aluminum in a Ti-Al compound or nanocluster. This is in contrast to the solvent-free samples, where NMR indicates that some aluminum is present in the form of  $\text{TiAl}_3$ , also consistent with XRD measurements.

This work suggests that variations in initial doping kinetics are likely due to the very different compound formation resulting from the doping conditions. The fact that sorption rates after many cycles tend to similar values for very many different dopant precursors and doping methods indicates that the initial compounds are likely transient, and may not be important in the ultimate sorption rates in Ti-doped sodium alanates.

## ACKNOWLEDGMENTS

This work was funded by the U.S. Department of Energy, Office of Power Technologies, Hydrogen Program Office under contract No. DE-AC36-83CH10093, and Sandia National Laboratories through the Laboratory Directed Research and

Development program. NMR work was performed under the auspices of the U.S. Department of Energy by University of California, Lawrence Livermore National Laboratory under Contract W-7405-Eng-48. The authors thank V. Ozolins for useful discussions and Ken Stewart for construction of the hydrogen sorption apparatus.

## References

- [1] B. Bogdanovic and M. Schwickardi. Ti-doped alkali metal aluminium hydrides as potential novel reversible hydrogen storage materials. *Journal of Alloys and Compounds*, 253-254(1-2):1 – 9, May 1997.
- [2] B. Bogdanovic, R.A. Brand, A. Marjanovic, M. Schwickardi, and J. Tolle. Metal-doped sodium aluminium hydrides as potential new hydrogen storage materials. *J. Al. Comp.*, 302(1-2):36 – 58, April 2000.
- [3] G. Sandrock, K. Gross, and G. Thomas. *Journal of Alloys and Compounds*, 339:299 – 308, June 2002.
- [4] E.H. Majzoub and K.J. Gross. Titanium-halide catalyst-precursors in sodium aluminum hydrides. *Journal of Alloys and Compounds*, 356-357:363 – 7, August 2003.
- [5] B. Bogdanovic, M. Felderhoff, M. Germann, M. Hartel, A. Pommerin, F. Schuth, C. Weidenthaler, and B. Zibrowius. *Journal of Alloys and Compounds*, 350:246 – 55, February 2003.
- [6] Dalin Sun, T. Kiyobayashi, H.T. Takeshita, N. Kuriyama, and C.M. Jensen. X-ray diffraction studies of titanium and zirconium doped NaAlH<sub>4</sub>: elucidation of doping induced structural changes and their relationship to enhanced hydrogen storage properties. *Journal of Alloys and Compounds*, 337:L8 – 11, May 2002.
- [7] C. Weidenthaler, A. Pommerin, M. Felderhoff, B. Bogdanovic, and F. Schuth. On the state of the titanium and zirconium in ti- or zr-doped naalh<sub>4</sub> hydrogen storage material. *PHYSICAL CHEMISTRY CHEMICAL PHYSICS*, 5(22):5149 – 5153, 2003.
- [8] K. J. Gross, E. H. Majzoub, and S. W. Spangler. The effects of titanium precursors on hydriding properties of alanates. *Journal of Alloys and Compounds*, 356/357:423 – 8, AUG 2003.
- [9] M. Fichtner, O. Fuhr, O. Kircher, and J. Rothe. Small ti clusters for catalysis of hydrogen exchange in naalh<sub>4</sub>. *NANO-TECHNOLOGY*, 14(7):778 – 785, JUL 2003.
- [10] B. Bogdanovic, M. Felderhoff, S. Kaskel, A. Pommerin, K. Schlichte, and F. Schuth. Improved hydrogen storage properties of ti-doped sodium alanate using titanium nanoparticles as doping agents. *ADVANCED MATERIALS*, 15(12):1012, JUN 2003.
- [11] Ritter H., Ihringer J., Maichle J.K., and Prandl W. *Simultaneous Structure Refinement with Multiple Powder Diffraction Data Sets*. Institute für Kristallographie der Universität Tübingen, Charlottenstr. 33, D-72070 Tübingen, 1998. Version 2.6.
- [12] V. Ozolins. Private communication.
- [13] C.J. Brinker and G.W. Scherer. *Sol-Gel Science*. Academic Press, 1989.
- [14] P. Florian, M. Gervais, A. Douy, D. Massiot, and J. P. Coutures. A multi-nuclear multiple-field nuclear magnetic resonance study of the ysub 2osub 3-alsub 2osub 3 phase diagram. *Journal of Physical Chemistry B*, 105(2):379 – 91, JAN 2001.